HHS Public Access

Author manuscript

Eur J Pharmacol. Author manuscript; available in PMC 2018 June 15.

Published in final edited form as:

Eur J Pharmacol. 2017 June 15; 805: 25–35. doi:10.1016/j.ejphar.2017.03.034.

A harmine-derived beta-carboline displays anti-cancer effects *in vitro* by targeting protein synthesis

Annelise Carvalho[a], **Jennifer Chu**[b], **Céline Meinguet**[c], **Robert Kiss**[a], **Guy Vandenbussche**[d], **Bernard Masereel**[c], **Johan Wouters**[c], **Alexander Kornienko**[e], **Jerry Pelletier**[b], and **Véronique Mathieu**[a,*]

[a]Laboratoire de Cancérologie et Toxicologie Expérimentale, Faculté de Pharmacie, Université Libre de Bruxelles, Brussels, Belgium

[b]Department of Biochemistry, McGill University, Montreal, Québec, Canada

[c]Namur Medicine and Drug Innovation Center (NAMEDIC-NARILIS), Université de Namur, Namur, Belgium

[d]Laboratory for the Structure and Function of Biological Membranes, Faculté des Sciences, Université Libre de Bruxelles, Brussels, Belgium

[e]Department of Chemistry and Biochemistry, Texas State University, 601 University Drive, San Marcos, TX 78666, USA

Abstract

Growing evidence indicates that protein synthesis is deregulated in cancer onset and progression and targeting this process might be a selective way to combat cancers. While harmine is known to inhibit DYRK1A and intercalate into the DNA, tri-substitution was shown previously to modify its activity profile in favor of protein synthesis inhibition. In this study, we thus evaluated the optimized derivative CM16 *in vitro* anti-cancer effects unfolding its protein synthesis inhibition activity. Indeed, the growth inhibitory profile of CM16 in the NCI 60-cancer-cell-line-panel correlated with those of other compounds described as protein synthesis inhibitors. Accordingly, CM16 decreased in a time- and concentration- dependent manner the translation of neosynthesized proteins *in vitro* while it did not affect mRNA transcription. CM16 rapidly penetrated into the cell in the perinuclear region of the endoplasmic reticulum where it appears to target translation initiation as highlighted by ribosomal disorganization. More precisely, we found that the mRNA expression levels of the initiation factors EIF1AX, EIF3E and EIF3H differ when comparing resistant or sensitive cell models to CM16. Additionally, CM16 induced eIF2α phosphorylation. Those effects could explain, at least partly, the CM16 cytostatic anti-cancer effects observed *in vitro* while neither cell cycle arrest nor DNA intercalation could be demonstrated. Therefore, targeting protein synthesis initiation with CM16 could represent a new promising alternative to current cancer therapies due to the specific alterations of the translation machinery in cancer cells

*Correspondence to: Laboratoire de Cancérologie et Toxicologie Expérimentale, Faculté de Pharmacie, Université Libre de Bruxelles [ULB], Campus de la Plaine, Boulevard du Triomphe, 1050 Brussels, Belgium. vemathie@ulb.ac.be (V. Mathieu).

Declaration of interests

The authors declare that they have no competing interests.

as recently evidenced with respect to EIF1AX and eIF3 complex, the potential targets identified in this present study.

Keywords

Beta-carboline; Harmine; Protein synthesis; Translation initiation; Cancer

1. Introduction

Among various processes that enable the continuous growth, multiplication and dissemination of malignant cells (Hanahan and Weinberg, 2011), protein synthesis plays an important role in the onset and progression of cancer. Growing evidence indicates that targeting mRNA translation as a cancer therapy has the potential of selectively eradicating cancerous cells (Bhat et al., 2015; Nasr and Pelletier, 2012; Spilka et al., 2013). In eukaryotic cells, mRNA trans lation occurs in four stages: initiation, elongation, termination and ribosome recycling. Among these, initiation is believed to be pivotal in the regulation of translation (Sonenberg and Hinnebusch, 2009), and is often altered in cancer through dysregulation of expression and/or phosphorylation status of translation initiation proteins, including eIF2α, eukaryotic translation initiation factor 3 (eIF3) and members of the eukaryotic translation initiation factor 4F complex (eIF4F) (Bhat et al., 2015; Blagden and Willis, 2011; Silvera et al., 2010). Translational control contributes to maintain several oncogenic programs (Silvera et al., 2010) and is reciprocally affected by oncogenic signaling pathways, which include MAPK and PI3K-AKT-mTOR (Bader et al., 2005; Topisirovic and Sonenberg, 2011). In response to energy and nutrient demand, mTOR is activated by the PI3K signaling cascade and promotes the assembly of the eIF4F complex resulting in the cap-dependent translation (Hay and Sonenberg, 2004; Ma and Blenis, 2009). Thus, the elevated activity of the translation machinery components and regulators makes them potential selective therapeutic targets to combat cancer cells (Bhat et al., 2015; Blagden and Willis, 2011; Malina et al., 2012).

Harmine, a natural β-carboline, is known to exert anticancer properties through i) the inhibition of DYRK1A (Göckler et al., 2009; Seifert et al., 2008), a protein kinase linked to tumorigenesis (Abbassi et al., 2015; Laguna et al., 2008; Pozo et al., 2013) and ii) DNA intercalating properties (Nafisi et al., 2010; Sarkar et al., 2014). Although displaying more potent growth inhibition than harmine itself, 2,7,9-*tri*-substituted β-carbolines exhibit no effect on DYRK1A, but instead were found to be possible protein synthesis inhibitors (Frédérick et al., 2012). Optimization of their pharmacological and physico-chemical properties led to the identification of CM16 as the lead compound, which to the best of our knowledge is the first harmine-derived beta-carboline (Meinguet et al., 2015) to be studied for its potential as protein synthesis inhibitor of cancer cells. The present study examines the anti-cancer properties of CM16 at the cellular level and on protein synthesis in three cancer cell models of different histological origins, i.e. the melanoma SKMEL-28, the glioma Hs683 and the breast cancer MDA-MB-231 models. We discovered EIF1AX and eIF3 complex members, recently identified as potential cancer targets, as possible regulators of cancer cell sensitivity to CM16.

2. Materials and methods

2.1. Cell lines and compounds

The human cancer cell lines, oligodendroglioma Hs683 (ATCC code HTB-138), melanoma SKMEL-28 (ATCC code HTB-72) and breast adenocarcinoma MDA-MB-231 (ATCC HTB26), as well as the normal human cell lines, skin fibroblasts NHDF (Lonza CC-2509), and lung fibroblasts NHLF (Lonza CC-2512) were selected for the current investigation. Cells were cultivated at 37 °C with 5% CO_2 in RPMI culture medium supplemented with 10% FBS, 200U penicillin-streptomycin, 0.1 mg/ml gentamicin and 4 mM L-glutamine, or fibroblast medium FBM supplemented with 2% fetal bovine serum, 0.1% insulin, rhFGF-B and gentamicin. MDA-MB-231 cells were cultured in DMEM supplemented with 10% FBS, 100 U/ml penicillin/streptomycin, and 2 mM L-glutamine at 37 °C and 5% CO_2. CM16 was synthetized as previously described (Meinguet et al., 2015).

2.2. MTT colorimetric assay

Cells were first grown in 96 well plates for 24 h and then treated with CM16 at different concentrations up to 100 μM or left untreated for 72 h. Viability was estimated by means of the MTT - (3-(4,5-dimethylthiazol- 2-yl)-2,5-diphenyl tetrazolium bromide (Sigma, Bornem, Belgium) mitochondrial reduction into formazan as previously described (Mosmann, 1983). Two experiments were performed in non-cancerous cell lines (NHDF and NHLF) and three in cancerous cell lines (Hs683, SKMEL-28 and MDA-MB-231), each in sextuplicate.

2.3. Quantitative videomicroscopy

Computer-assisted phase contrast microscopy was performed as previously described (Debeir et al., 2008). Briefly, Hs683, SKMEL-28 or MDA-MB-231 cells were seeded in 25 cm^2 culture flasks and left untreated or treated with CM16 at their GI_{50} concentrations determined with the MTT colorimetric assay or at the concentration 10 times higher. Pictures of one field were taken every four min during a 72 h period and further compiled into a short movie (Debeir et al., 2008). Quantitatively, global growth ratio was determined based on cell counting of pictures corresponding to 24 h, 48 h and 72 h in comparison to 0 h. Experiments were performed once in triplicates.

2.4. Fluorescence assays

2.4.1. CM16 cell penetration and distribution analysis—The fluorescence properties of CM16 were first determined in a phosphate buffer at pH 7.4 as ex/em: 330/439 nm. To qualitatively analyze the CM16 cell penetration and distribution, tumor cells (Hs683, SKMEL-28 and MDA-MB-231) were seeded on glass coverslips in cell culture plates and, after attachment, treated with 5 μM CM16 or left untreated. For imaging of the living cells, medium was removed and PBS was added. Coverslips were rapidly transferred to a slide and images were captured with the Imager M2 fluorescence microscope (Carl Zeiss, Zaventem, Belgium) coupled with the AxioCam ICm1 and AxioImager software (Carl Zeiss, Zaventem, Belgium). The experiment was conducted twice in duplicate and three images per condition were taken.

2.4.2. Ribosome fluorescent staining—Endoplasmic reticulum (ER) staining of cells was performed with glibenclamide ER-tracker red dye (Molecular Probes - Life Technologies, Merelbeke, Belgium) by fluorescence microscopy. Cells were seeded on coverslips in cell culture plates and left untreated or treated with CM16 after attachment (at least 24 h). Following treatment, the dye solution (1 μM in PBS) was incubated with the samples for 30 min at 37 °C. The staining solution was replaced with cell culture medium and sample-containing coverslips were transferred to microscope slides. The imaging of living cells was performed similarly to description above (item a) with fluorescence microscope (Carl Zeiss, Zaventem, Belgium). Experiments were conducted once or twice, depending on the cell line, in duplicate and five images per condition were taken.

2.5. Protein neosynthesis evaluation

2.5.1. Fluorescence method—To evaluate the effects of CM16 on neosynthesized proteins the Click-iT AHA alexa fluor 488 kit (Invitrogen, Life Technologies, Merelbeke, Belgium) was used. A methionine analog L-azidohomoalanine is incorporated in newly synthesized proteins and reacts with an alkyne coupled to alexa 488 fluorescent dye allowing measurement (ex/em: 495/520 nm). Hs683, SKMEL-28 and NHDF cells were seeded in 96 wells plates and left untreated or treated with CM16 or positive control, i.e. cycloheximide (Santa Cruz Biotech., Heidelberg, Germany). The treatment was followed by the addition of L-azidohomoalanine (1/1000) for four h. After fixation with formaldehyde, the neosynthesized proteins were stained according to the manufacturer's recommendations. Normalization according to cell number was carried out as described in the user manual with Hoescht counterstaining. The fluorescent signal was measured in a microplate reader (SynergyMX Biotek, Winooski, USA: ex/em: 350/460 nm). Experiments were performed each in sextuplicate.

2.5.2. ^{35}S Methionine incorporation—MDA-MB-231 or NHDF cells were seeded (50,000 cells per well in a 12 well plate format) one day prior to the labeling experiment. On the day of the experiment, cells were incubated with CM16 at the indicated concentrations for a total of 1 h and 20 min. During the last 20 min, [^{35}S]-methionine/cysteine (150–200 μCi/ml) (Perkin Elmer, Waltham, MA) was added to the cells. At the end of the incubation, cells were washed twice with ice-cold PBS and labeling reactions were terminated through the addition of RIPA buffer. Newly synthesized radiolabeled proteins were precipitated on 3 MM Whatman paper (pre-blocked with 0.1% L-methionine) using trichloroacetic acid (TCA) and washed twice with 5% TCA, followed by two washes of ethanol. Samples were then dried and quantitated using scintillation counting. CPMs were normalized to total protein, which was determined using the DC Assay (Bio-rad). Experimental results represent three biological replicates, each performed in technical duplicate.

2.6. Investigation of the translation initiation: ribosome and polysome organization study

Ribosomes and polysomes were separated through ultracentrifugation in sucrose gradient, as described in Cencic et al. (2007). Briefly, Hs683, SKMEL-28, NHDF, NHLF cells were seeded in cell culture flasks and left untreated (negative control) or treated with puromycin or CM16. Cells were then scraped and collected in a PBS buffer containing 100 μg/ml cycloheximide and centrifuged (400×*g*, 4 °C, 10 min). Pellets were resuspended in a

hypotonic lysis buffer (5 mM Tris pH 7,5; 2,5 mM $MgCl_2$; 1,5 mM KCl), supplemented with cycloheximide 100 μg/ml, DTT 2 mM, 5 μL RNasin Ribonuclease Inhibitor (Promega, Leiden, Netherlands), 10 μL of 10% Triton X-100 and 10 μL of 10% sodium deoxycholate. Samples were centrifuged (16100 rcf, 2 min, 4 °C) and loaded onto a 10 – 50% sucrose gradient and centrifuged for 2 h at 156,213×*g* at 4 °C (SW 60 Ti rotor, Beckman, Ramsey, USA). The obtained gradients were then collected in fractions through a constant pump flow and absorbance measurement carried out at 264 nm in a microplate reader (SynergyMX Biotek, Winooski, USA). Three independent experiments were carried out in the Hs683 and SKMEL-28 cancer cell lines and one experiment in the non-cancerous non-transformed fibroblasts NHLF and NHDF.

For the polysomes generated using MDA-MB-231 cells, samples were loaded onto a 10–50% sucrose gradient and centrifuged for 2 h and 15 min at 217,290×*g*. The gradients were then fractionated while reading UV_{254} absorbance using the Foxy® R1 fraction collector (Teledyne, ISCO). One experiment (or measurements) was performed.

2.7. Immunodetection

MDA-MB-231 or NHDF cells were treated with the indicated concentrations of CM16 for 60 min and lysates were collected by washing the cells with ice cold PBS followed lysis using a buffer composed of 20 mM HEPES [pH 7.5], 150 mM NaCl, 1% Triton-X100, 10% glycerol, 1 mM EDTA, 10 mM tetrasodium pyrophosphate, 100 mM NaF, 17.5 mM β-glycerophosphate, 1 mM PMSF, 4 mg/ml aprotinin, and 2 mg/ml pepstatin A. Samples were resolved on a 10% NuPAGE gel and transferred to a PVDF membrane (BioRad) for immunoblotting. The following antibodies were used in this study: eukaryotic elongation factor 2 (eEF2) (#9742, Cell Signaling), pan eIF2α (#9722, Cell Signaling), phospho-eIF2α (Ser51) (#9721, Cell Signaling). Two independent experiments were performed.

2.8. NCI data analysis

NCI GI_{50} profile of CM16 was compared to those of the compounds in the NCI database with the COMPARE software tool of the NCI (Paull et al., 1989). Only the compounds displaying a COMPARE correlation coefficient (CCC) with CM16 above 0.7 were considered in Table 1.

2.9. Statistical analysis

For the transcriptomic comparison, we selected the models with GI_{50} >1 μM or <0.1 μM as the least versus the most sensitive models of the NCI 60 cancer cell line panel. A list of potential candidates regulating or involved in protein synthesis was established based on the literature and includes the main components of the cap-dependent translation machinery, as well as kinases and important proteins involved in the protein synthesis pathways (Table 1 in Carvalho et al. (2017)). Comparison of the two groups was performed by T-test comparison of the Z score with the Statistica Software. Z scores are provided by the NCI and are determined for each probe/cell line pair by the subtraction from its intensity in the transcriptomic array of the probe mean across the 60 cell lines, and division by the standard deviation of the probe (across the 60 cell lines). The z score average was then calculated as the mean across all probes and probe sets that passed quality control criteria.

3. Results

3.1. Evaluation of in vitro global growth inhibition by CM16

CM16 (Fig. 1) was evaluated at the National Cancer Institute (NCI – Bethesda, USA) in the 60 cancer cell line panel. Fig. 2A shows that the mean 50% growth inhibitory concentration (GI_{50}) obtained by the NCI is ~0.2 μM and varies from <0.01 to 4 μM. Of note, 80% of the cell lines display GI_{50} close to the mean value, between 0.1 and 0.5 μM (Fig. 2A). The mean 50% lethal concentration (LC_{50}) in the NCI panel is 9 μM and ranges from 0.5 to >100 μM (Fig. 2B). Interestingly, the response profiles of the 60 cell lines based on the GI_{50} values differ from those obtained with the LC_{50} counterparts. For example, for the leukemia sub-panel these differential sensitivities are opposite to each other. These observations indicate that CM16 exerts cytostatic activity at lower concentrations (close to GI_{50}) through different mechanism(s) from that associated with its cytotoxic effects at higher concentrations (close to LC_{50}). Because CM16 does not display specificity towards one defined cancer type in the NCI panel, we decided to use cancer cell models of distinct origins, i.e., glioma (Hs683), melanoma (SKMEL-28) and breast carcinoma (MDA-MB-231), for the current investigation to limit cell-type specific and context-dependent factors. Moreover, while keeping the same sensitivity to CM16 effects, these three cell lines display different sensitivity to apoptosis – SKMEL-28 being apoptosis-resistant (Mathieu et al., 2009), while Hs683 (Branle et al., 2002) and MDA-MB-231 (Syed Alwi et al., 2012) are apoptosis-sensitive. We also included in our assay non-transformed cells, i.e. dermal and lung fibroblasts. The mean GI_{50} was about an order of magnitude lower in cancer cell cultures than in non-cancerous models (i.e. 0.3 μM versus 3.8 μM respectively; Fig. 3A) indicating moderate selectivity towards cancer cells. Importantly, our mean GI_{50} of 0.3 μM on cancer cells (Fig. 3A) is similar to the one of the NCI (GI_{50}: 0.2 μM).

3.2. CM16 exerts in vitro anticancer activity through cytostatic effects

The cytostatic activity of CM16 was confirmed by means of quantitative videomicroscopy in glioma Hs683, melanoma SKMEL-28 and MDAMB-231 breast cancer cells using the MTT-derived GI_{50} concentrations as illustrated morphologically and quantitatively (Fig. 3B–C). We further investigated the cytostatic effects of CM16 at its GI_{50} using flow cytometric cell cycle analysis but did not observe any significant effect as previously shown (Fig. 1A–B in Carvalho et al. (2017)). Thus, CM16-induced growth inhibition is not related to a specific cell cycle phase or arrest. Accordingly, we observed that CM16 and its previously studied analogues (Frédérick et al., 2012) do not interact with DNA when assayed *in vitro* (data not shown), as opposed to harmine and related compounds that display DNA intercalating and groove binding properties (Nafisi et al., 2010; Sarkar et al., 2014).

3.3. CM16 cellular penetration and distribution

Fluorescent properties of CM16 were used to study its cellular penetration and distribution by fluorescence microscopy. CM16 appeared to penetrate as early as 5 min after initiating treatment (Fig. 4A) in the perinuclear region, while the nucleus itself remained unstained even after 6 h of treatment (data not shown). Moreover CM16 appeared to co-localize with the endoplasmic reticulum (Fig. 4B–D for Hs683, SKMEL-28 and MDA-MB-231, respectively), where the translation machinery is assembled. However, no obvious

differences were revealed in cell penetration or distribution of CM16 between non-transformed fibroblasts and cancer cells that could ex plain, even partly, the selectivity we observed above (data not shown).

3.4. CM16 inhibits protein synthesis

To evaluate whether CM16 could be a protein synthesis inhibitor, its NCI GI_{50}-based cellular sensitivity profile was compared to those of >765,000 compounds in the NCI database using the COMPARE algorithm (Paull et al., 1989). Among 11 compounds, displaying a COMPARE correlation coefficient (CCC) with CM16 above 0.7, mechanistic information was available for 8 (Pubmed or the SCOPUS database as of September 2016), of which 6 have been described as potential protein synthesis inhibitors (Table 1). Moreover, significant correlation (CCC of 0.71) was found with **5a**, one of the previously studied analogues of CM16 (Table 1) (Frédérick et al., 2012). Consequently, we investigated the effects of CM16 on newly synthesized proteins in transformed Hs683, SKMEL-28 and MDAMB-231 and in NHDF non-transformed cell lines (Fig. 5A–D). Hs683 and SKMEL-28 cells were treated with 0.5 and 5.0 μM of CM16 from 1 to 6 h, treatment schedules that induced cytostatic effects only, as verified by videomicroscopy (Fig. 3C). At 5 μM, the neosynthesized protein level was decreased by 50% after only a 1 h treatment in SKMEL-28 cells and 3 h in HS683 cells and the inhibition was concentration-dependent. At 0.5 μM, the treatment period had to be increased from 6 to 24 h to obtain a similar decrease (data not shown). Similarly, we observed a concentration-dependent decrease in incorporated ^{35}S methionine in MDA-MB-231 breast cancer cells after only 80 min of treatment with CM16, with the concentration of 10 μM leading to nearly a complete inhibition of protein synthesis (Fig. 5D). Evaluation of newly synthesized proteins in NHDF normal fibroblast cells showed no significant different response than cancer cell model (Fig. 5C and D). We also envisaged effects at the transcription level but no alteration of the incorporation of a nucleotide analog into the newly-transcribed mRNA for up to 24 h and in the presence of up to 5.0 μM CM16 in Hs683 and SKMEL-28 cells lines could be observed (Fig. 2A–B (Carvalho et al., 2017)). We concluded that CM16 does not inhibit transcription while it does inhibit mRNA translation, at least as a common feature across the different cellular models used in the present study.

3.5. CM16 affects ribosomal organization in cancer cells

To investigate the effects of CM16 on translation further, we evaluated the ribosomal assembly into 80S functional subunit and polysome organization by means of sucrose gradients. CM16 induced the accumulation of 80S ribosomes in treated cells, while polysomes decreased after 80 min of treatment at 10 μM (the concentration that completely inhibited ^{35}S methionine incorporation in 80 min) in MDA-MB-231 (Fig. 6A). We confirmed that ribosomal organization in Hs683 and SKMEL-28 cells was affected as early as after a 3 h treatment with lower concentrations, i.e. 0.5 and 5.0 μM CM16 (Fig. 6B–C). Again, we observed an accumulation of the fractions corresponding to the free 80S ribosome when compared to puromycin-induced effects (Fig. 6B). Non-transformed fibroblasts also displayed similar altered profiles but at high concentrations only (Fig. 6D–E).

Because actin plays critical roles in translation initiation and proper polysome organization (Gross and Kinzy, 2007), fluorescent staining of fibrillary actin was performed in the absence or presence of 0.5 and 5.0 μM of CM16 over a 24 h period but no significant modification was noticed, at least in Hs683 and SKMEL-28 (data not shown).

3.6. Initiation factors are involved in CM16-induced inhibition of mRNA translation

Because the previous chemical series were shown to modify the eIF2α expression and activity levels (Frédérick et al., 2012), we further investigated if CM16 could affect mRNA translation by eIF2α targeting. Its phosphorylation was observed in MDA-MB-231 cells when treated with 2.5 and 10 μM of CM16 for 80 min, an effect also found in NHDF cells (Fig. 7A). To further evaluate whether the expression level of eIF2α and its partners eIF2β and eIF2γ could drive, at least partly, the sensitivity of cells to CM16, we utilized the NCI cell line transcriptomic characterization.[1] Indeed, although the GI_{50} values of CM16 in the majority of the NCI cell line panel are close to the average of 0.2 μM (Fig. 2A), and without large variation, four cell lines appeared poorly sensitive to CM16 with GI_{50} >1 μM (least sensitive, LS) while five other appeared highly sensitive, i.e. those with a GI_{50} <0.1 μM (most sensitive, MS). We thus compared the transcriptomic expression levels of eIF2α and its partners eIF2β and eIF2γ between these two groups of cell lines displaying two orders of magnitude difference of sensitivity to CM16 but no statistical significance could be observed (Fig. 7B). Eukaryotic translation initiation factor 2 alpha kinase 3 (PERK) is a key kinase regulating eIF2α phosphorylation (Ron, 2002) and thus activity. However, CM16 did not alter PERK kinase activity *in vitro* as shown in Fig. 3 in Carvalho et al. (2017). We then extended the comparison of the highly versus poorly sensitive cell lines of the NCI to a more extensive list of 57 components, actors and regulators of translation (Table 1 in Carvalho et al. (2017)). Interestingly among these 57 targets of the translation machinery selected, only three initiation factors were found to be significantly differentially expressed between the two groups: EIF1AX, EIF3E and EIF3H (Fig. 7C), while neither elongation nor signaling pathways investigated were different (data not shown). The expression level of initiation factors could thus drive, at least partly, the sensitivity of a cell line to CM16 and further support the effects of this compound on the initiation phase of translation.

4. Discussion

Malignant cells require higher levels of protein synthesis to maintain several oncogenic programs (Silvera et al., 2010) and in recent years it has been extensively shown that several distinct dysregulations of the translation process occur in cancer cells (Nasr and Pelletier, 2012; Ruggero, 2013; Spilka et al., 2013). Direct inhibitors of the translation machinery, targeting the eIF4F, eIF3 or the ternary complexes, are under investigation at different stages of development (for a detailed review of therapeutic inhibitors of translation in cancer, see (Bhat et al., 2015)). Efforts toward this goal also include the development of inhibitors of upstream signaling pathways (e.g., PI3K-mTOR and MNK) (Bhat et al., 2015; Blagden and Willis, 2011; Malina et al., 2012). Our research aimed at the elucidation of the anti-cancer

[1]We did not perform proteomic comparison of these cell lines because some data were missing for several targets and cell lines rendering the analysis impossible to interpret.

potential of a preclinical candidate CM16, a β-carboline derived from a harmala alkaloid harmine (Meinguet et al., 2015), which was investigated herein as a protein synthesis inhibitor *in vitro*.

First, we observed that CM16 exerts cytostatic effects at its GI_{50} concentration in cancer cells (Figs. 2A and 3B-C) and that it displays at least 10 times more selectivity in inhibiting the growth of cancer cells as compared to non-cancerous cell lines (Fig. 3A). Although cytostatic, CM16 did not induce any cell cycle phase arrest, which is consistent with the lack of its interaction with DNA as well as the absence of CM16 localization to the nucleus (Fig. 4A).

We compared the growth inhibitory profile of CM16 in the 60 NCI cancer cell line panel to those of the existing compounds in the NCI database using the COMPARE software, which expresses and ranks the similarities in the differential cellular sensitivities as the Pearson correlation coefficient (Paull et al., 1989). This approach has been successfully employed to identify new inhibitors of translation in the past (Chan et al., 2004) and it indeed supported CM16 as a protein synthesis inhibitor.

Further, the inhibition of translation induced by CM16 in different cancer models, such as melanoma, glioma and breast cancer cell lines, was found to be time- and concentration-dependent while no effect on transcription was observed. These results are consistent with the parallel intracellular distribution of CM16 with the endoplasmic reticulum (Fig. 4B–D), the major site for mRNA translation (Reid and Nicchitta, 2015). Importantly, because no selectivity against a cancer type appeared in the NCI panel, we conducted the assays in cancer cell models from different origins, i.e. glioma, melanoma and breast cancer cell lines to avoid cell-type and context-dependent limitations. In fact, CM16 appeared to affect translation initiation as illustrated by ribosomal disorganization in the three cancer cell models used while those effects were observed at higher doses only in the non-cancerous models. Translation initiation is dependent on the formation of eIF4F complex (eIF4G, eIF4A and eIF4E), which recruits the 40S ribosomal unit, and the ternary complex (eIF2, $tRNA^{met}$ and GTP), necessary for initiation. Previous beta-carboline compound series was shown to decrease eIF2α expression and/or phosphorylation levels (Frédérick et al., 2011). In this study, preliminary data obtained with breast cancer cells indicate that CM16 could induce eIF2α phosphorylation (Fig. 7A), which will in turn compromise the formation of the ternary complex and binding of $tRNA^{met}$ to the ribosome (Hinnebusch and Lorsch, 2012), and thus inhibit protein synthesis (Koromilas, 2015).

Compared to harmine derivatives previously characterized, compound CM16 is less hydrophobic and does not bear large substituents like phenyl or cyclohexyl rings. At the present stage of our investigations, it is however difficult to link differences in eIF2α activity within this series and specific stereoelectronic properties and, thus, no convincing (Q)SAR can be proposed. A family of four kinases – eukaryotic translation initiation factor 2 alpha kinase 1 (HRI), eukaryotic translation initiation factor 2 alpha kinase 2 (PKR), eukaryotic translation initiation factor 2 alpha kinase 4 (GCN2) and PERK – regulates eIF2α phosphorylation (Koromilas, 2015; Ron, 2002; Wek et al., 2006). While no direct effect of CM16 on PERK kinase activity *in vitro* could be evidenced (see Fig. 3 in Carvalho et al.

(2017)) it remains possible that CM16 acts, at least partly, through ER stress-mediated activation of PERK in cellular assay (Koromilas, 2015) and/or via the other kinases mentioned above.

CM16 selectivity towards cancer cells was observed through the *in vitro* evaluation of growth inhibition (Fig. 3A). We also observed that CM16-induced ribosomal disorganization was present but less pronounced in non-cancerous cell models (Fig. 6D–E). Interestingly, targeting initiation proteins instead of elongation ones would offer greater selectivity in inhibiting the growth of cancer cells as elongation inhibitors seem to have a narrow therapeutic window due to the inhibition of global protein synthesis of non-transformed cells (Lindqvist et al., 2009; Malina et al., 2012). Moreover, several initiation proteins are dysregulated in cancer cells as compared to normal cells. As CM16 induces phosphorylation of eIF2-α similarly in cancerous and non-cancerous cells (Fig. 7A), it is unlikely that the effects on this initiation factor are responsible for the selectivity observed. Also, no difference in cell penetration and distribution of CM16 between non-cancerous and cancerous models could be found to explain this selectivity. Therefore, we extended the study to 57 genes involved in translation initiation and elongation or in their control using the transcriptomic characterization of the NCI 60 cell line panel. Among these 57 targets (see Table 1 in Carvalho et al. (2017)), the mRNA levels of only three initiation factors, i.e. EIF1AX, EIF3E and EIF3H, were found to be significantly different in highly sensitive cancer cell lines compared to those with low sensitivity towards CM16 (Fig. 7C). eIF1A, the protein encoded by EIF1AX, is important in the formation of the pre-initiation complex, composed of the 40S subunit, eukaryotic translation initiation factor 1 (eIF1), eukaryotic translation initiation factor 5 (eIF5), eIF3 and the ternary complex (Bhat et al., 2015; Spilka et al., 2013), and together with eIF1, is required for mRNA scanning and binding at the initiation codon (Spilka et al., 2013). Mutations in the EIF1AX gene have been associated with tumor development and progression in thyroid cancer (Jung et al., 2016; Landa et al., 2016) uveal melanomas (Decatur et al., 2016; Field et al., 2016) and possibly ovarian tumor carcinogenesis (Hunter et al., 2015). Knowledge of its functional roles in cancer biology is still currently limited (Spilka et al., 2013) and warrant further investigations. Similarly, eIF3e and eIF3h have been both reported to be dysregulated in cancer (Bhat et al., 2015). They are part of the largest initiation complex, i.e. the eIF3 complex, which is composed of 10–13 subunits acting together in the initiation process. Their main roles include recruitment of the mRNA to the 40S ribosomal unit and stabilizing the ternary complex (Bhat et al., 2015; Spilka et al., 2013). At the protein level, eIF3e affects proliferation and survival of glioblastoma cells (Sesen et al., 2014), is involved in colon tumor progression (Li et al., 2014) and breast tumor formation, (Suo et al., 2015) progression (Grzmil et al., 2010) and metastasis (Gillis and Lewis, 2013). High levels of eIF3h maintain the malignancy of several cancer cell lines *in vitro* (Zhang et al., 2008) and have been indeed observed in breast, prostate and hepatocellular carcinomas (Hershey, 2015; Zhu et al., 2016). How the targeting of these initiation factors help to explain superior activity of CM16 against cancerous over non-cancerous cells remains to be investigated.

5. Conclusion

Translation inhibition in cancer is emerging as a new and promising alternative to the existing therapies due to the specific alterations of the translation machinery in cancer cells. The results of the present investigation show that CM16, a preclinical candidate derived from a harmala alkaloid harmine with favorable drug-like physico-chemical characteristics, inhibits cancer cell protein synthesis at the mRNA translation level via perturbation of their ribosomal organization. EIF1AX and EIF3 complex members, recently reported to be involved in cancer onset and progression, were found in the present study to be differentially expressed in cancer cell lines depending on their sensitivity towards CM16.

Acknowledgments

The PhD of A.C. is financially supported by the Coordenação de Aperfeiçoamento de Pessoal de Nivel Superior (Grant 0674-13/3; CAPES; Brazil). C.M. acknowledges the grant from the *Télévie* (FRS-FNRS; Belgium). R.K. is a director of research with the Fonds National de la Recherche Scientifique (FRS-FNRS; Belgium) that supported the present project (#3.4525.11: Anti-cancéreux dérivés de l'harmine from 2010 to 2014). Part of this study is also supported by the grant by the Belgian Brain Tumor Support (BBTS; Belgium). JP acknowledges grants from the Canadian Institutes of Health Research (MOP-106530 and MOP-115126). A.K. acknowledges the National Cancer Institute (CA186046-01A1) and Welch Foundation (AI-0045). The sources of funding had no role in the design of the study or in the collection, analysis, and interpretation of data or in writing the manuscript. Funding provided grant salaries to PhD students (AC and CM) and support for the consumables of the current work. We thank Mohsin Mssassi for his help during his stay in the Laboratoire of Cancérologie et Toxicologie Expérimentale (ULB, Belgium).

Abbreviations

DYRK1A	dual specificity tyrosine phosphorylation regulated kinase 1A
EIF1AX	eukaryotic translation initiation factor 1A, X-linked
EIF3E	eukaryotic translation initiation factor 3 subunit E
EIF3H	eukaryotic translation initiation factor 3 subunit H
eIF2α	eukaryotic translation initiation factor 2 subunit 1

References

Abbassi R, Johns TG, Kassiou M, Munoz L. DYRK1A in neurodegeneration and cancer: molecular basis and clinical implications. Pharmacol Ther. 2015; 151:87–98. [PubMed: 25795597]

Bader AG, Kang S, Zhao L, Vogt PK. Oncogenic PI3K deregulates transcription and translation. Nat Rev Cancer. 2005; 5:921–929. [PubMed: 16341083]

Bannon PG, Dawes J, Dean RT. Malformin A prevents IL-1 induced endothelial changes by inhibition of protein synthesis. Thromb Haemost. 1994; 72:482–483. [PubMed: 7531879]

Beutler JA, Kang M-I, Robert F, Clement JA, Pelletier J, Colburn NH, McKee TC, Goncharova E, McMahon JB, Henrich CJ. Quassinoid inhibition of AP-1 function does not correlate with cytotoxicity or protein synthesis inhibition. J Nat Prod Prod. 2009; 72:503–506.

Bhat M, Robichaud N, Hulea L, Sonenberg N, Pelletier J, Topisirovic I. Targeting the translation machinery in cancer. Nat Rev Drug Discov. 2015; 14:261–278. [PubMed: 25743081]

Blagden SP, Willis AE. The biological and therapeutic relevance of mRNA translation in cancer. Nat Rev Clin Oncol. 2011; 8:280–291. [PubMed: 21364523]

Branle F, Lefranc F, Camby I, Jeuken J, Geurts-Moespot A, Sprenger S, Sweep F, Kiss R, Salmon I. Evaluation of the efficiency of chemotherapy in in vivo orthotopic models of human glioma cells

with and without 1p19q deletions and in C6 rat orthotopic allografts serving for the evaluation of surgery combined with chemotherapy. Cancer. 2002; 95:641–655. [PubMed: 12209758]

Carvalho A, Chu J, Meinguet C, Kiss R, Vandenbussche G, Masereel B, Wouters J, Kornienko A, Pelletier J, Mathieu V. Data in support of a harmine-derived beta-carboline in vitro effects in cancer cells through protein synthesis. Data Brief. 2017 (submitted for publication).

Cencic R, Robert F, Pelletier J. Identifying small molecule inhibitors of eukaryotic translation initiation. Methods Enzymol. 2007; 431:269–302. [PubMed: 17923239]

Chan J, Khan SN, Harvey I, Merrick W, Pelletier J. Eukaryotic protein synthesis inhibitors identified by comparison of cytotoxicity profiles. RNA. 2004; 10:528–543. [PubMed: 14970397]

Chitnis MP, Alate AD, Menon RS. Effect of bouvardin (NSC 259968) on the growth characteristics an nucleic acids and protein syntheses profiles of P388 leukemia cells. Chemotherapy. 1981; 27:126–130. [PubMed: 7471902]

Debeir O, Mégalizzi V, Warzée N, Kiss R, Decaestecker C. Videomicroscopic extraction of specific information on cell proliferation and migration in vitro. Exp Cell Res. 2008; 314:2985–2998. [PubMed: 18598694]

Decatur CL, Ong E, Garg N, Anbunathan H, Bowcock AM, Field MG, Harbour JW. Driver mutations in uveal melanoma: associations with gene expression profile and patient outcomes. JAMA Ophthalmol. 2016; 134:728–733. [PubMed: 27123562]

Dobretsov S, Tamimi Y, Al-Kindi MA, Burney I. Screening for anti-cancer compounds in marine organisms in Oman. Sultan Qaboos Univ Med J. 2016; 16:e168–e174. [PubMed: 27226907]

Field MG, Durante MA, Decatur CL, Tarlan B, Oelschlager KM, Stone JF, Kuznetsov J, Bowcock AM, Kurtenbach S, Harbour JW. Epigenetic reprogramming and aberrant expression of PRAME are associated with increased metastatic risk in Class 1 and Class 2 uveal melanomas. Oncotarget. 2016; 7:59209–59219. [PubMed: 27486988]

Frédérick R, Bruyére C, Vancraeynest C, Reniers J, Meinguet C, Pochet L, Backlund A, Masereel B, Kiss R, Wouters J. Novel trisubstituted harmine derivatives with original in vitro anticancer activity. J Med Chem. 2012; 55:6489–6501. [PubMed: 22770529]

Garreau de Loubresse N, Prokhorova I, Holtkamp W, Rodnina MV, Yusupova G, Yusupov M. Structural basis for the inhibition of the eukaryotic ribosome. Nature. 2014; 513:517–522. [PubMed: 25209664]

Gillis LD, Lewis SM. Decreased eIF3e/Int6 expression causes epithelial-to-mesenchymal transition in breast epithelial cells. Oncogene. 2013; 32:3598–3605. [PubMed: 22907435]

Gladstone M, Frederick B, Zheng D, Edwards A, Yoon P, Stickel S, DeLaney T, Chan DC, Raben D, Su TT. A translation inhibitor identified in a Drosophila screen enhances the effect of ionizing radiation and taxol in mammalian models of cancer. Dis Model Mech. 2012; 5:342–350. [PubMed: 22344740]

Göckler N, Jofre G, Papadopoulos C, Soppa U, Tejedor FJ, Becker W. Harmine specifically inhibits protein kinase DYRK1A and interferes with neurite formation. FEBS J. 2009; 276:6324–6337. [PubMed: 19796173]

Gross SR, Kinzy TG. Improper organization of the actin cytoskeleton affects protein synthesis at initiation. Mol Cell Biol. 2007; 27:1974–1989. [PubMed: 17178834]

Grzmil M, Rzymski T, Milani M, Harris AL, Capper RG, Saunders NJ, Salhan A, Ragoussis J, Norbury CJ. An oncogenic role of eIF3e/INT6 in human breast cancer. Oncogene. 2010; 29:4080–4089. [PubMed: 20453879]

Hagimori K, Fukuda T, Hasegawa Y, Omura S, Tomoda H. Fungal malformins inhibit bleomycin-induced G2 checkpoint in Jurkat cells. Biol Pharm Bull. 2007; 30:1379–1383. [PubMed: 17666789]

Hanahan D, Weinberg Ra. Hallmarks of cancer: the next generation. Cell. 2011; 144:646–674. [PubMed: 21376230]

Hay N, Sonenberg N. Upstream and downstream of mTOR. Genes Dev. 2004; 18:1926–1945. [PubMed: 15314020]

Hershey JWB. The role of eIF3 and its individual subunits in cancer. Biochim Biophys Acta - Gene Regul Mech. 2015; 1849:792–800.

Hinnebusch AG, Lorsch JR. The mechanism of eukaryotic translation initiation - new insights and challenges.pdf. Cold Spring Harb Perspect Biol. 2012; 4:a011544. [PubMed: 22815232]

Hsu CW, Chuang SM, Wu WL, Hou MH. The crucial role of divalent metal ions in the DNA-acting Efficacy and inhibition of the transcription of dimeric Chromomycin A3. PLoS One. 2012; 7:e43792. [PubMed: 22984445]

Hunter SM, Anglesio MS, Ryland GL, Sharma R, Chiew Y, Rowley SM, Doyle MA, Li J, Gilks CB, Moss P, Allan PE, Stephens AN, Huntsman DG, DeFazio A, Bowtell DD, Gorringe KL, Campbell IG. Australian Ovarian Cancer Study Group. Molecular profiling of low grade serous ovarian tumours identifies novel candidate driver genes. Oncotarget. 2015; 6:37663–37677. [PubMed: 26506417]

Jung S, Kim MS, Jung CK, Park H, Kim Y, Liu J, Bae J, Lee SH, Kim T, Lee H, Chung Y. Mutational burdens and evolutionary ages of thyroid follicular adenoma are comparable to those of follicular carcinoma. Oncotarget. 2016; 7:69638–69648. [PubMed: 27626165]

Koizumi Y, Fukudome H, Hasumi K. Fibrinolytic activation promoted by the cyclopentapeptide malformin: involvement of cytoskeletal reorganization. Biol Pharm Bull. 2011; 34:1426–1431. [PubMed: 21881228]

Koromilas AE. Roles of the translation initiation factor eIF2α serine 51 phosphorylation in cancer formation and treatment. Biochim Biophys Acta - Gene Regul Mech. 2015; 1849:871–880.

Laguna A, Aranda S, Barallobre MJ, Barhoum R, Fernández E, Fotaki V, Delabar JM, de la Luna S, de la Villa P, Arbonés ML. The protein kinase DYRK1A regulates Caspase-9-mediated apoptosis during retina development. Dev Cell. 2008; 15:841–853. [PubMed: 19081073]

Landa I, Ibrahimpasic T, Boucai L, Sinha R, Knauf JA, Shah RH, Dogan S, Ricarte-Filho JC, Krishnamoorthy GP, Xu B, Schultz N, Berger MF, Sander C, Taylor BS, Ghossein R, Ganly I, Fagin JA. Genomic and transcriptomic hallmarks of poorly differentiated and anaplastic thyroid cancers. J Clin Investig. 2016; 126:1052–1066. [PubMed: 26878173]

Li X, Bin Xie F, Liu SS, Li Y, Zhou JC, Liu YQ, Yuan HQ, Lou HX. Naphtho-γ-pyrones from endophyte Aspergillus niger occurring in the liverwort Heteroscyphus tener (Steph.) Schiffn Chem. Biodivers. 2013; 10:1193–1201.

Li Z, Lin S, Jiang T, Wang J, Lu H, Tang H, Teng M, Fan J. Overexpression of eIF3e is correlated with colon tumor development and poor prognosis. Int J Clin Exp Pathol. 2014; 7:6462–6474. [PubMed: 25400724]

Lindqvist L, Pelletier J, Sciences MM, Sir P, Osler W, Rosalind T, Centre GC. Inhibitors of translation initiation as cancer therapeutics. Future Med Chem. 2009; 1:1709–1722. [PubMed: 21425987]

Liu Y, Wang M, Wang D, Li X, Wang W, Lou H, Yuan H. Malformin A1 promotes cell death through induction of apoptosis, necrosis and autophagy in prostate cancer cells. Cancer Chemother Pharmacol. 2015; 77:63–75. [PubMed: 26645406]

Ma XM, Blenis J. Molecular mechanisms of mTOR-mediated translational control. Nat Rev Mol Cell Biol. 2009; 10:307–318. [PubMed: 19339977]

Malina A, Mills JR, Pelletier J. Emerging therapeutics targeting mRNA translation. Cold Spring Harb Perspect Biol. 2012; 4:a012377. [PubMed: 22474009]

Mathieu V, Pirker C, Martin de Lassalle E, Vernier M, Mijatovic T, DeNeve N, Gaussin J-F, Dehoux M, Lefranc F, Berger W, Kiss R. The sodium pump α1 sub-unit: a disease progression-related target for metastatic melanoma treatment. J Cell Mol Med. 2009; 13:3960–3972. [PubMed: 19243476]

Meinguet C, Bruyère C, Frédérick R, Mathieu V, Vancraeynest C, Pochet L, Laloy J, Mortier J, Wolber G, Kiss R, Masereel B, Wouters J. 3D-QSAR, design, synthesis and characterization of trisubstituted harmine derivatives with in vitro antiproliferative properties. Eur J Med Chem. 2015; 94:45–55. [PubMed: 25747498]

Miller SC, Huang R, Sakamuru S, Shukla SJ, Attene-Ramos MS, Shinn P, Van Leer D, Leister W, Austin CP, Xia M. Identification of known drugs that act as inhibitors of NF-kappaB signaling and their mechanism of action. Biochem Pharmacol. 2010; 79:1272–1280. [PubMed: 20067776]

Mir MA, Dasgupta D. Association of the anticancer antibiotic chromomycin A 3 with the nucleosome: role of core histone tail domains in the binding process. Biochemistry. 2001; 40:11578–11585. [PubMed: 11560508]

Mosmann T. Rapid colorimetric assay for cellular growth and survival: application to proliferation and cytotoxicity assays. J Immunol Methods. 1983; 65:55–63. [PubMed: 6606682]

Nafisi S, Bonsaii M, Maali P, Khalilzadeh MA, Manouchehri F. β-carboline alkaloids bind DNA. J Photochem Photobiol B Biol. 2010; 100:84–91.

Nasr Z, Pelletier J. Tumor progression and metastasis: role of translational deregulation. Anticancer Res. 2012; 32:3077–3084. [PubMed: 22843876]

Paull KD, Shoemaker RH, Hodes L, Monks A, Scudiero DA, Rubinstein L, Boyd MR, Plowman J. Display and analysis of patterns of differential activity of drugs against human tumor cell lines: development of mean graph and COMPARE algorithm. J Natl Cancer Inst. 1989; 81:1088–1092. [PubMed: 2738938]

Pozo N, Zahonero C, Fernández P, Liñares JM, Ayuso A, Hagiwara M, Pérez A, Ricoy JR, Hernández-Laín A, Sepúlveda JM, Sánchez-Gómez P. Inhibition of DYRK1A destabilizes EGFR and reduces EGFR-dependent glioblastoma growth. J Clin Invest. 2013; 123:2475–2487. [PubMed: 23635774]

Reid DW, Nicchitta CV. Diversity and selectivity in mRNA translation on the endoplasmic reticulum. Nat Rev Neurosci. 2015; 16:221–231.

Ron D. Translational control in the endoplasmic reticulum stress response. J Clin Investig. 2002; 110:1383–1388. [PubMed: 12438433]

Ruggero D. Translational control in cancer etiology. Cold Spring Harb Perspect Biol. 2013; 5:a012336. [PubMed: 22767671]

Sarkar S, Pandya P, Bhadra K. Sequence specific binding of beta carbolinealkaloid harmalol with deoxyribonucleotides: binding Heterogeneity, conformational, thermodynamic and cytotoxic aspects. PLoS One. 2014; 9:e108022. [PubMed: 25247695]

Seifert A, Allan La, Clarke PR. DYRK1A phosphorylates caspase 9 at an inhibitory site and is potently inhibited in human cells by harmine. FEBS J. 2008; 275:6268–6280. [PubMed: 19016842]

Sesen J, Cammas A, Scotland SJ, Elefterion B, Lemarié A, Millevoi S, Mathew LK, Seva C, Toulas C, Moyal ECJ, Skuli N. Int6/eIF3e is essential for proliferation and survival of human glioblastoma cells. Int J Mol Sci. 2014; 15:2172–2190. [PubMed: 24481065]

Silvera D, Formenti SC, Schneider RJ. Translational control in cancer. Nat Rev Cancer. 2010; 10:254–266. [PubMed: 20332778]

Sonenberg N, Hinnebusch AG. Regulation of translation initiation in eukaryotes: mechanisms and biological targets. Cell. 2009; 136:731–745. [PubMed: 19239892]

Spilka R, Ernst C, Mehta AK, Haybaeck J. Eukaryotic translation initiation factors in cancer development and progression. Cancer Lett. 2013; 340:9–21. [PubMed: 23830805]

Stickel SA, Gomes NP, Frederick B, Raben D, Su TT. Bouvardin is a radiation modulator with a novel mechanism of action. Radiat Res. 2015; 184:392–403. [PubMed: 26414509]

Suo J, Medina D, Herrera S, Zheng Z-Y, Jin L, Chamness GC, Contreras A, Gutierrez C, Hilsenbeck S, Umar A, Foekens Ja, Hanash S, Schiff R, Zhang X, Chang EC. Int6 reduction activates stromal fibroblasts to enhance transforming activity in breast epithelial cells. Cell Biosci. 2015; 5:1–10. [PubMed: 25601894]

Syed Alwi SS, Cavell BE, Donlevy A, Packham G. Differential induction of apoptosis in human breast cancer cell lines by phenethyl isothiocyanate, a glutathione depleting agent. Cell Stress Chaperon-. 2012; 17:529–538.

Tan Q-W, Gao F-L, Wang F-R, Chen Q-J. Anti-TMV activity of malformin A1, a cyclic penta-peptide produced by an endophytic fungus Aspergillus tubingensis FJBJ11. Int J Mol Sci. 2015; 16:5750–5761. [PubMed: 25775156]

Topisirovic I, Sonenberg N. mRNA translation and energy metabolism in cancer: the role of the MAPK and mTORC1 Pathways. Cold Spring Harb Symp Quant Biol. 2011; LXXVI:355–367.

Toume K, Tsukahara K, Ito H, Arai M, Ishibashi M. Chromomycins A2 and A3 from marine actinomycetes with TRAIL resistance-overcoming and Wnt signal inhibitory activities. Mar Drugs. 2014; 12:3466–3476. [PubMed: 24905484]

Wek RC, Jiang H-Y, Anthony TG. Coping with stress: eIF2 kinases and translational control. Biochem Soc Trans. 2006; 34:7–11. [PubMed: 16246168]

Zalacaín M, Zaera E, Vázquez D, Jiménez A. The mode of action of the antitumor drug bouvardin, an inhibitor of protein synthesis in eukaryotic cells. FEBS Lett. 1982; 148:95–97. [PubMed: 6924616]

Zhan J, Gunaherath GMKB, Wijeratne EMK, Gunatilaka aaL. Asperpyrone D and other metabolites of the plant-associated fungal strain Aspergillus tubingensis. Phytochemistry. 2007; 68:368–372. [PubMed: 17150233]

Zhang L, Smit-McBride Z, Pan X, Rheinhardt J, Hershey JWB. An oncogenic role for the phosphorylated h-subunit of human translation initiation factor eIF3. J Biol Chem. 2008; 283:24047–24060. [PubMed: 18544531]

Zhu Q, Qiao G, Zeng X, Li Y, Yan J, Duan R, Zhi-Young D. Elevated expression of eukaryotic translation initiation factor 3H is associated with proliferation, invasion and tumorigenicity in human hepatocellular carcinoma. Oncotarget. 2016; 7:49888–49901. [PubMed: 27340783]

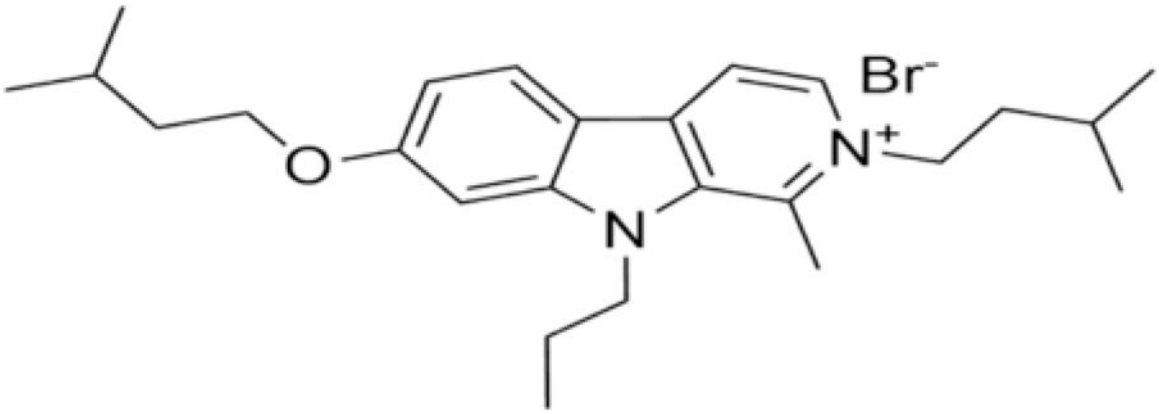

Fig. 1.
Chemical structure of the β-carboline derivative CM16.

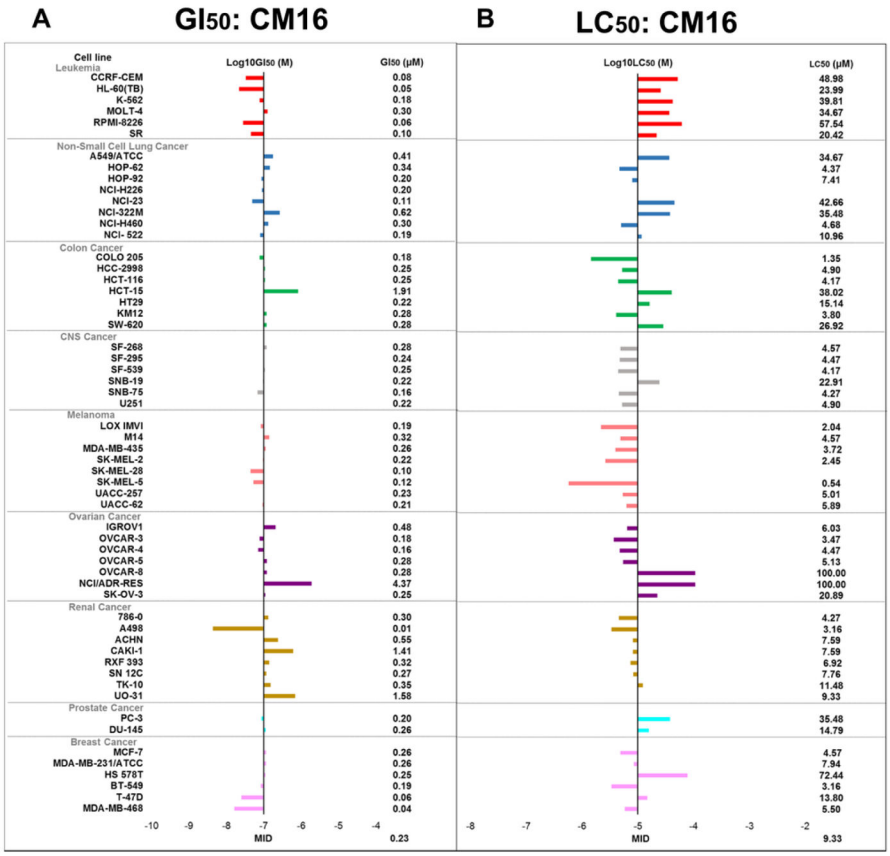

Fig. 2.

In vitro anti-cancer effects of CM16 in the NCI 60-cell line panel. (Adapted presentation - shown with the permission of the NCI) A: Global growth inhibition [GI_{50}] of each cell line after 48 h of culture with CM16. "-7" represents the mean GI_{50} of the 60 cell lines, i.e. 0.2 μM. Log_{10} differences are represented by the bars. B: Lethal concentration [LC_{50}] of CM16 for each cell line compared to the mean LC_{50} ["-5"]. The scale of the bars is in log_{10} as for A and B.

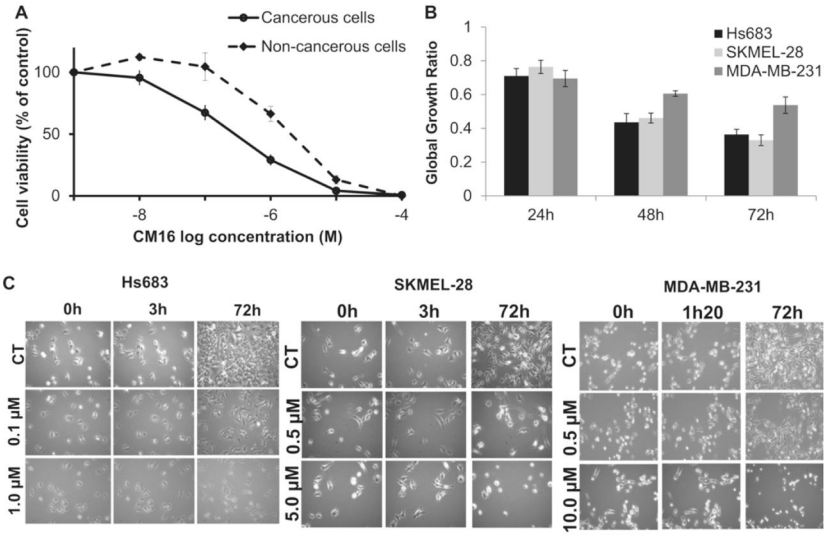

Fig. 3. CM16-induced cytostatic growth inhibition effects in cancer cells

A: Cell growth inhibition in cancer cells (solid line) versus non-cancerous cells (dashed line) treated with CM16 for 72 h. Cancerous cell lines: Hs683, SKMEL-28 and MDA-MB-231. Non-cancerous cell lines: NHLF and NHDF non-transformed fibroblasts. Data are expressed as the mean of viable cells relative to control (100%)±S.E.M. of the six replicates of one representative experiment. **B:** Global growth ratio in HS683, SKMEL-28 and MDA-MB-231 cells after 24 h, 48 h and 72 h treatments with CM16 at their GI_{50}. Results are expressed as the mean growth ratio between treated cells relative to control (1)±S.E.M. of three replicates of one representative experiment. **C:** Videomicroscopy of CM16-induced *in vitro* effects in Hs683, SKMEL-28 and MDA-MB-231. Figures are representative of one experiment performed in three replicates.

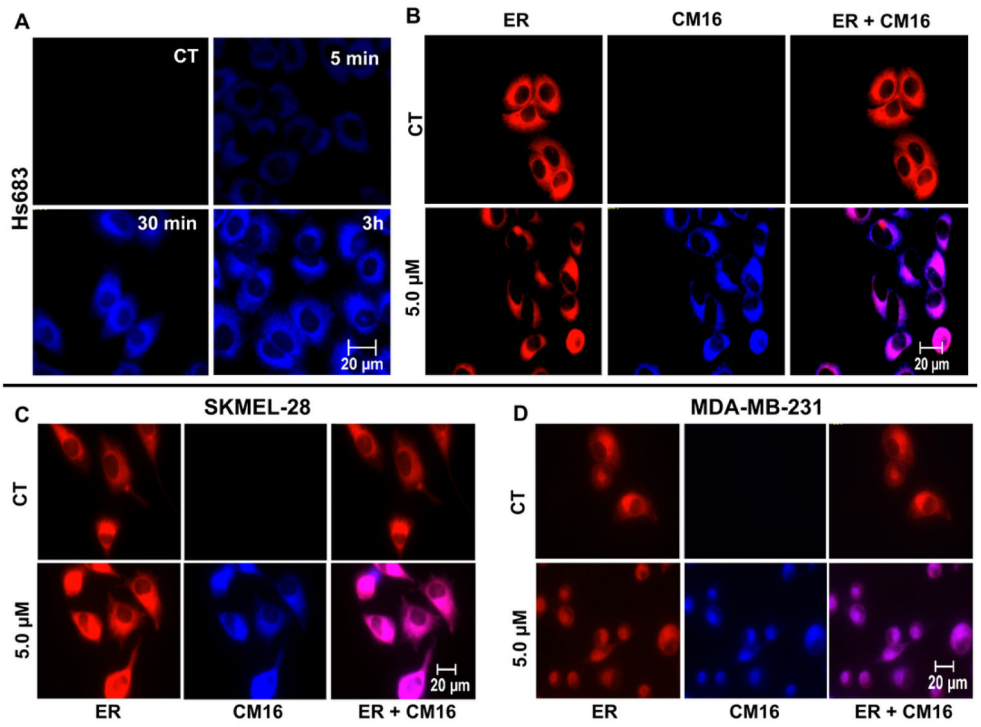

Fig. 4. CM16 cellular penetration and distribution in the ER and protein synthesis inhibitio

A: CM16 fluorescence properties allow its visualization in blue color (filter ex/em: 359–371/397 nm) in Hs683 cells over time after 5 µM treatment. **B:** CM16 parallel distribution to the endoplasmic reticulum fluorescent probe (ER-tracker) after a 3 h treatment in Hs683, **C:** SKMEL-28 and **D**: MDA-MB-231 cell lines. Exposure times for blue filter (ex/em) 359–371/397 nm: 40 ms (SKMEL-28) and 80 ms (Hs683 and MDA-MB-231); and for red filter (ex/em) 540–580/593–668 nm: 283 ms (SKMEL-28) and 850 ms (Hs683 and MDA-MB-231). All pictures were taken with a 40× objective. Illustrations are representative of one experiment performed in two replicates.

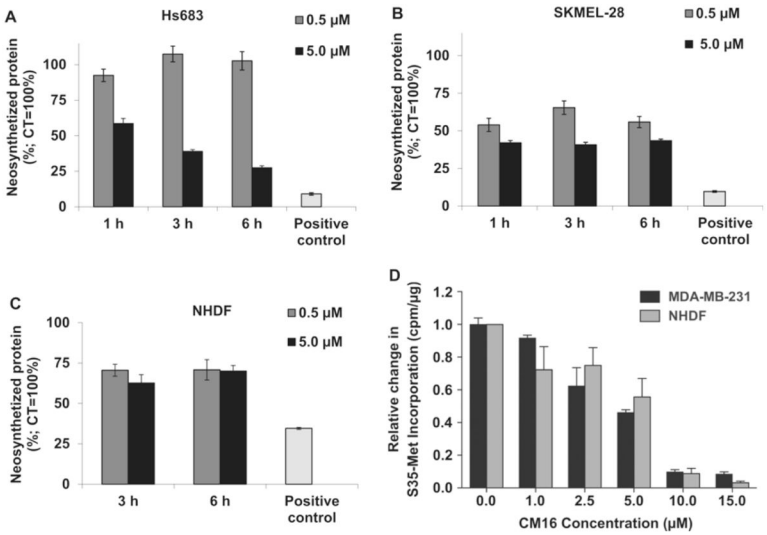

Fig. 5.

Analysis of the newly synthesized proteins in **A:** Hs683 and, **B:** SKMEL-28 and **C:** NHDF cells by fluorescent assay. Positive control: cycloheximide 0.1 mM for 1 h. Data are expressed as the mean neosynthezised protein amounts normalized to the control (100%) ±S.E.M. of the six replicates of one representative experiment. **D**: Dose-dependent evaluation of **[**^{35}S]-methionine labeling in MDA-MB-231and NHDF cells after 80 min of treatment. CPMs were normalized to total protein.

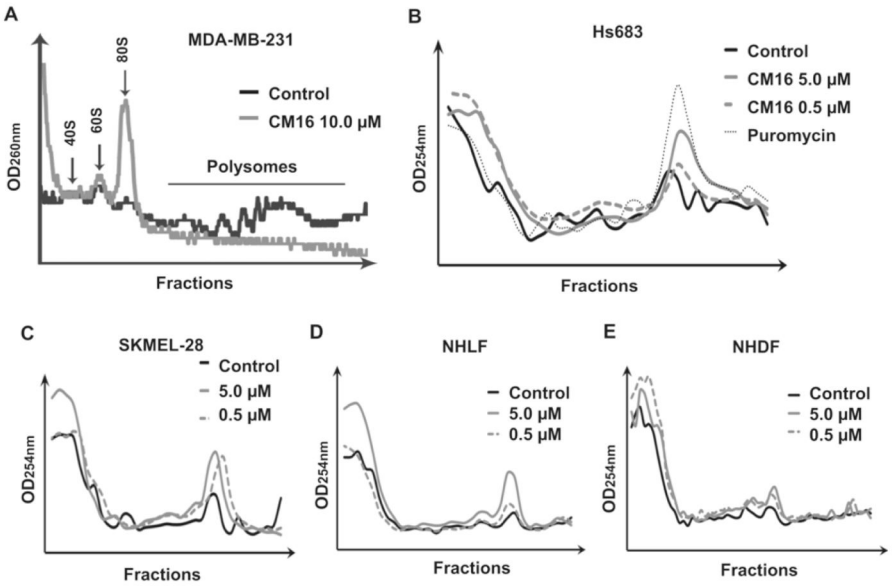

Fig. 6. CM16 effects on ribosomal organization by sucrose gradient analysis

Effect of CM16 on ribosomal units and polysome organization after treatment. **A:** MDA-MB-231 cells incubated for 80 min with CM16 at 10 µM in comparison to the control. **B:** Cancerous cell lines Hs683 and **C:** SKMEL-28 and non-cancerous cell lines **D:** NHDF and **E:** NHLF incubated with CM16 at 0.5 µM or 5.0 µM for 3 h (grey lines) in comparison to the control (solid black line). Puromycin was used as positive control (1 h, 184 µM) to visualize the 80S peak containing fractions. Three or one independent experiments were performed, depending on the cell line. Each profile is representative of one experiment.

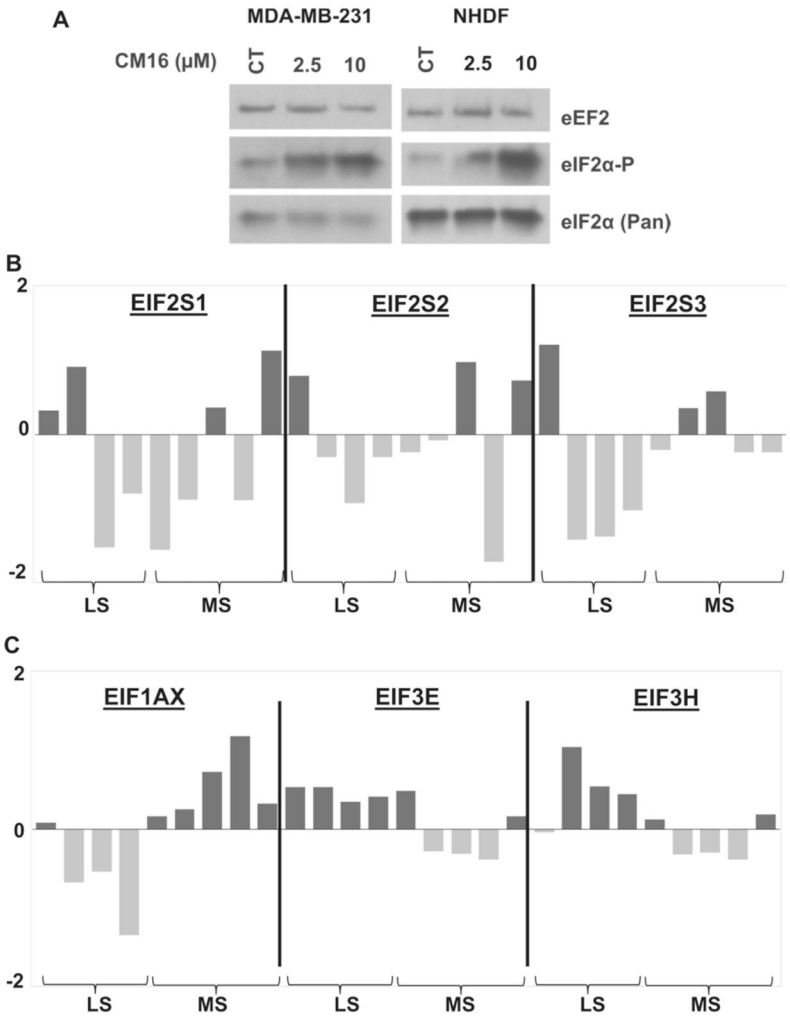

Fig. 7. Initiation factors study

A: Effects of CM16 on the expression and phosphorylation status of eIF2α in MDA-MB231 cancerous and NHDF non-cancerous cells by western blot. Representative western blot of two experiments. **B and C**: Comparison of the transcriptomic expression levels of main translation initiation genes in the most (MS) versus least sensitive (LS) cell lines to CM16 effects among the NCI-cell-line-panel screening. The four least sensitive cell lines (i.e. those with a GI_{50} >1 μM) are HCT-15 [−5.72], NCI/ADR-RES [−5.36], Caki-1 [−5.85] and UO-31 [−5.80]. The five most sensitive cell lines (i.e. with a GI_{50} <0.1 μM) are A498 [−8.00], HL60 [−7.30], CCRF-CEM [−7.12], RPMI-8226 [−7.19] and T47D [−7.23]. **B:** Transcriptomic comparison of eIF2α, β and γ subunits between the most and least sensitive cell lines to the CM16 growth inhibitory effects identified in the NCI cell line panel. **C:** Transcriptomic comparison of the targets with significantly different expression levels between the cell lines most and least sensitive to CM16 growth inhibitory effects identified in the NCI cell line panel by means of *t*-test comparison. Increased expression levels as compared to the 60 cell line mean appear in black while decreased expression levels appear in grey. Results are expressed as Z scores as provided by the NCI database. Z scores are determined for each probe/cell line pair by the subtraction from its intensity of the probe

mean (across the 60 cell lines), and division by the standard deviation of the probe (across the 60 cell lines). The z score average was then calculated as the mean across all probes and probe sets that passed quality control criteria.

Table 1

Correlations of CM16 with protein synthesis inhibitors in the NCI 60-Cell-Line Screen using the COMPARE Algorithm.

Compound	Correlation CM16 (NSC 779185)	Information	References
NSC 656902	0.744	Quassinoid tested by NCI among other quassionoids that were protein synthesis inhibitors	Beutler et al. (2009)
PHYLLANTHOSIDE,S3′-DESACETYL – NSC 342443	0.723	Protein synthesis inhibitor (Phyllanthoside - NSC 328426)	Chan et al. (2004); Garreau de Loubresse et al. (2014)
CHROMOMYCIN A3 – NSC 58514	0.722	1. Protein synthesis inhibitor 2. NF-kappaB inhibitor +effect on estrogen receptor 3. Effect on TRAIL and Wnt signaling pathways	1. Chan et al. (2004); Hsu et al. (2012); Mir and Dasgupta (2001) 2. Miller et al. (2010) 3. Toume et al. (2014)
MALFORMIN A – NSC 324646	0.713	1. Protein synthesis inhibitor (preventing IL-1 induced endothelial changes) 2. Effect on cell cycle 3. Fibrinolytic activity 4. Activity against cancerous cell lines 5. Cytotoxic effect on cancerous cell lines 6. Anti-Tobacco mosaic virus	1. Bannon et al. (1994) 2. Hagimori et al. (2007) 3. Koizumi et al. (2011) 4. Dobretsov et al. (2016); Li et al. (2013); Zhan et al. (2007) 5. Liu et al. (2015) 6. Tan et al. (2015)
5a – NSC 760180	0.713	Protein synthesis inhibitor	Frédérick et al. (2012)
BOUVARDIN – NSC 259968	0.707	Protein synthesis inhibitor	Chitnis et al. (1981); Gladstone et al. (2012); Stickel et al. (2015); Zalacaín et al. (1982)